

# Image-Based Measurement of Structural Color using Spectral Camera

Kazuki Iwata, Hiroki Shirasawa, Keita Hirai;

Department of Imaging Sciences, Chiba University; 1-33, Yayoicho, Inage Ward, Chiba-shi, Chiba, 263-8522 Japan.

## Abstract

We perceive structural colors by optical phenomena such as light interference and diffraction caused by a fine structure of the object surface. One of the characteristics of structural colors is that a wavelength distribution of light changes depending on an incident angle of a light source and a viewing angle. Generally, for color evaluation and reproduction, it is required to acquire reflection characteristics of objects. Therefore, BRDF (Bidirectional Reflectance Distribution Function) is often used as a function that represents reflection characteristics depending on incident and viewing angles. In this study, we measured BRDF of structural colors based on a method to acquire image-based material reflection characteristics using a spectral camera. The measurement was performed by aligning an optical axis of a spectral camera with a structural color sample and changing an irradiation angle of a light source. Reflection characteristics were represented by using a radiance factor, which was a ratio between a spectral radiance of white material and that of structural color. From measurement results, we confirmed an angle-dependent radiance factor. Finally, based on a measured spectral radiance of a structural color sample, we spectrally reproduced the structural color using a spectral projector based on model fitting of spectral data.

## Introduction

A Standard color appearance depends on a surface spectral reflectance of objects. On the other hand, structural colors are not caused by a surface reflectance of objects. Color appearance of incident light on microstructure surfaces depends on optical phenomena such as interference, diffraction, and scattering inside a structure. Actual example objects of structural colors are thin-film interference phenomena in soap bubbles, multi-layer interference phenomena in Buprestidae, and diffraction phenomena in compact discs. One of the characteristics of structural colors is that a wavelength distribution differs depending on an incident angle of a light source and a viewing angle, which allows us to perceive different colors depending on where we are focusing.

It is crucial to acquire a surface reflection characteristic of material when evaluating and reproducing the color of the material. For achieving this goal, BRDF (Bidirectional Reflectance Distribution Function) is widely used as a function that represents reflection characteristics depending on material angles [1-3]. Even for structural colors, it is essential to acquire BRDF in order to represent reflection characteristics and physical appearance with angle dependencies. When acquiring BRDF of structural colors, a goniophotometer is usually used [4]. In this measurement method, angular sampling is very dense, and structural color can be measured with high accuracy. However, there is a drawback that the amount of data is enormous, and it takes time.

On the other hand, several reproductions and manipulation methods for structural color have been proposed. N. Okada et al.

analyzed an optical simulation of wings of a morpho butterfly with multiple optical properties by the FDTD (Finite Difference Time Domain) method and rendered it [5]. L. Belcour et al. proposed a CG reproduction model of structural colors of a thin film whose thickness can be changed arbitrarily [6]. S. Werner and his colleague reproduced iridescent colors caused by a scratch by wave optics rendering [7]. T. Auzinger et al. manufactured a free-form sub-micrometer structure by the direct laser writing method called multiphoton lithography, and it became possible to design any structural colors [8]. However, studies on effective structural color measurement methods have not been actively addressed.

In this study, based on the method of acquiring image-based material reflection property [9], we propose a measurement method using a spectral camera and implement a simple method for measuring structural colors. Also, we verify and interpolate reflection characteristics of structural colors spectroscopically, considering angle dependence for modeling structural colors. As an application, we spectrally reproduce data of structural color samples measured using a spectral projector [10].

## A simple method for measuring structural color

### Measurement environment

Figure 1 shows the structural color samples used in this study. We prepared two types of stainless oxidative coloring (Nakano Chemical). The shape of the samples is a cylinder with radius  $R = 34$  mm. As shown in Fig.1, the samples include significant specular characteristics such as mirrors because the structural color samples were generated by coating stainless surfaces. A camera used a 2D spectral radiance meter (2D spectral camera) TOPCON SR-5000. The resolution of the camera is  $1376 \times 1024$  pixels. In an actual measurement, in order to speed up processing, we measured a range of  $400 \times 100$  pixels, which includes the entire width of the sample. In this case, the actual resolution to an object surface was  $0.170 \times 0.170$  mm per pixel. The wavelength range was from 380 nm to 780 nm (5 nm interval). As a light source, we used an incandescent light bulb (Iwasaki Electric) as a point light source. Figure 2 shows the measurement environment. Measurement was performed in a dark room so that light from the surroundings would not enter the sample.

Figure 3 shows the geometry setup in the measurement experiments. The distance between the sample center and camera  $dc$  was 434 mm, and the distance between the sample and light source  $dl$  was 475 mm. In this study, we used the structural color samples of coated stainless surfaces, which include mirror-like specular reflectance. Then, we focused on the measurement of specular angles. As the results, the light source irradiation angle  $\theta_L$  was set to  $-20^\circ, -25^\circ, -30^\circ, -35^\circ, -40^\circ, -45^\circ$ . A protractor was used to measure the angle. The measurement was performed on the tape-shaped white imitation paper wrapped around the sample in advance. The intensity of reflected light varies depending on the location of the sample, and captured images appear

overexposed and underexposed, so images were taken at multiple exposure times (in other words, HDR), and then the data was combined.

### Measurement angle processing

For incident angle and viewing angle processing, we applied the coordinate system based on Ref. [9]. By treating the light source as a point light source and the camera as a pinhole camera, it is possible to treat each position of the sample as a pair of different incident and viewing angles. From the coordinate system in Figure 3, let any pixel in the x-direction of a captured image be point P on the cylinder. The light source vector  $P_L$ , camera vector  $P_C$ , and normal vector n at point P are as follows.

$$\begin{aligned} P_L &= [(d_L \cos \theta_L - R \cos \theta_S), (d_L \sin \theta_L - R \sin \theta_S)], \\ P_C &= [(d_C - R \cos \theta_S), (0 - R \sin \theta_S)], \end{aligned} \quad (1)$$

$n = (\cos \theta_S, \sin \theta_S)$ , where,  $\theta_S = \sin^{-1}(x_n/R)$ , and  $x_n = (\text{Pixel position in } x\text{-direction} - \text{Central pixel position in } x\text{-direction}) \times \text{resolution}$ . From Eq.(1) the incident and viewing angles,  $\theta_i$  and  $\theta_o$ , at point P are as follows,

$$\theta_i = \cos^{-1} \frac{P_L \cdot n}{|P_L|}, \theta_o = \cos^{-1} \frac{P_C \cdot n}{|P_C|} \quad (2)$$

Figure 4 shows the sampling range of incident and viewing angles. As shown in Fig.5, incident (viewing) angles from the left side of the normal line n are described in positive notation, and incident (viewing) angles from the right side are described in negative notation. As described above, we focused on the measurement of specular angles, because we used structural color samples of coated stainless surfaces, which include mirror-like specular reflectance.



Figure 1. Structural color sample of blue (left), green (right)

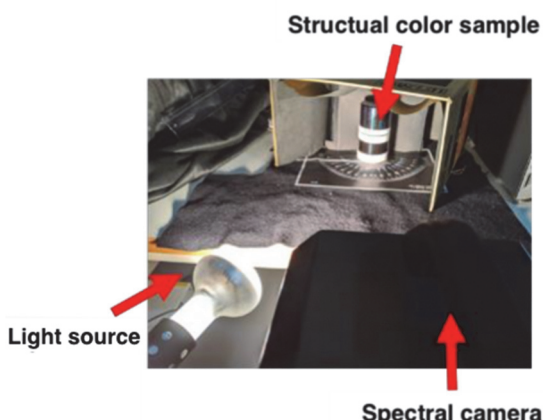


Figure 2. Measurement environment

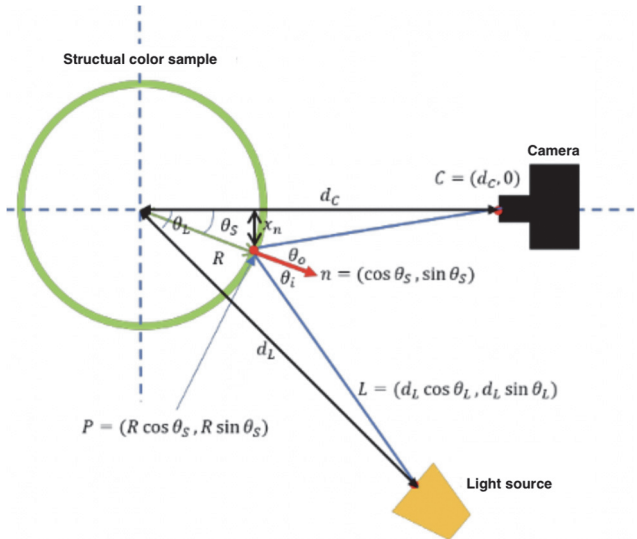


Figure 3. Geometry setup in measurement experiments

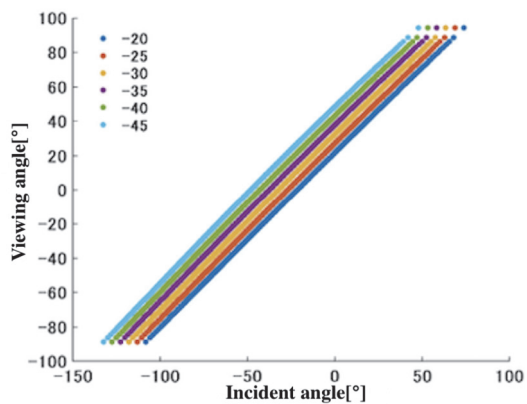


Figure 4. Sampling range of incident and viewing angles

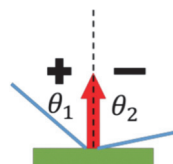


Figure 5. Angle description

In this study, reflection characteristics are expressed by emissivity. The emissivity is expressed by the radiance factor  $\beta$ , which is a ratio of the spectral radiance of the structural color sample  $L_{\text{sample}}$  to the spectral radiance of the white imitation paper  $L_{\text{white}}$  on the same y-axis.

$$\beta(\theta_i, \theta_o, \lambda) = \frac{L_{\text{sample}}(\theta_i, \theta_o, \lambda)}{L_{\text{white}}(\theta_i, \theta_o, \lambda)} \quad (3)$$

### Measurement results and discussions

Figure 6 shows the measured radiance factor of two types of the samples at the viewing angle  $\theta_o = 12.5^\circ$ . From Fig.6, both samples show a high radiance factor when close to regular reflection ( $\theta_i = -12.5^\circ$ ), while a radiance factor is tiny when far from regular reflection. Since the samples used for the measurement have a structure in which a thin film is spread on a stainless-steel base, it shows a characteristic peculiar to metal that a specular reflection component becomes high. From Fig.6, the

green sample has a spectral distribution with a peak at 550 nm to 600 nm, and the blue sample have a spectral distribution with a peak at 450 nm to 500 nm. This measurement accurately captured the spectral distribution of the actual color of the samples. However, the samples used for our measurements have a considerable difference between a radiance factor at angles close to regular reflection and angles far from regular reflection. Therefore, change in angle dramatically affects the colors.

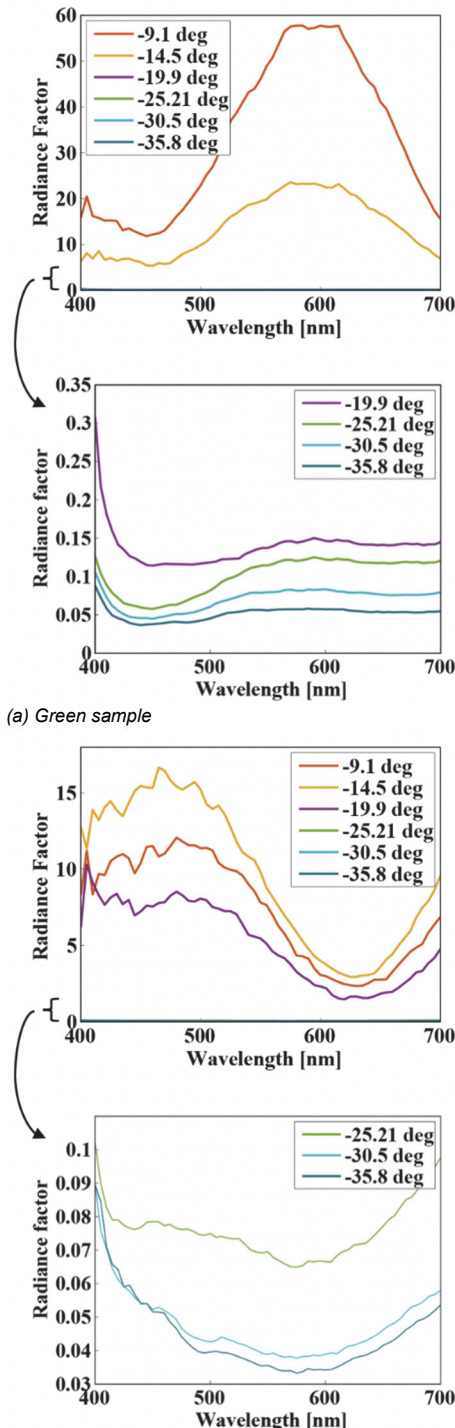


**Figure 6.** Measured radiance factor for various incident angles at the viewing angle  $\theta_o = 12.5^\circ$ . The bottom figures of (a) and (b) are the close up of the low radiance factor level of the upper side figures. The measurement data from -19.9 to -35.8 degrees exists around zero in the upper side figures.

## Model fitting to measurement results

Since there are few angular samplings of the measured radiance factor, model fitting was performed for reflections across the normal line to interpolate the angular samplings. Several types of researches addressed to modeling structural colors [6, 7]. However, in our measurement, a radiance factor is higher as an angle is closer to regular reflection. In this case, a conventional modeling technique cannot be applied. Therefore, we used a simple Gaussian fitting for modeling the measured angle-dependent data as follows:

$$\alpha * \exp \left\{ \frac{(x_{in} - x_{out})^2}{2\beta} \right\} \quad (4)$$

Equation (4) is a Gaussian function with a peak at the regular (specular) reflection, with  $x_{in}$  (incident angle) and  $x_{out}$  (viewing angle) as variables. Since Eq.(4) does not have a wavelength as a variable, Gaussian fitting was performed for each wavelength to estimate the parameters  $\alpha$  and  $\beta$ . In order to confirm the approximate accuracy of the proposed Gaussian function, the average RMSE (Root Mean Square Error) between the measured value of all angles and the predicted value of the model at reflection across the normal line was calculated. As a result, the RMSE of the green sample was 1.70, and the blue sample was 0.97. It can be seen from the numerical values that the proposed model can be approximated.

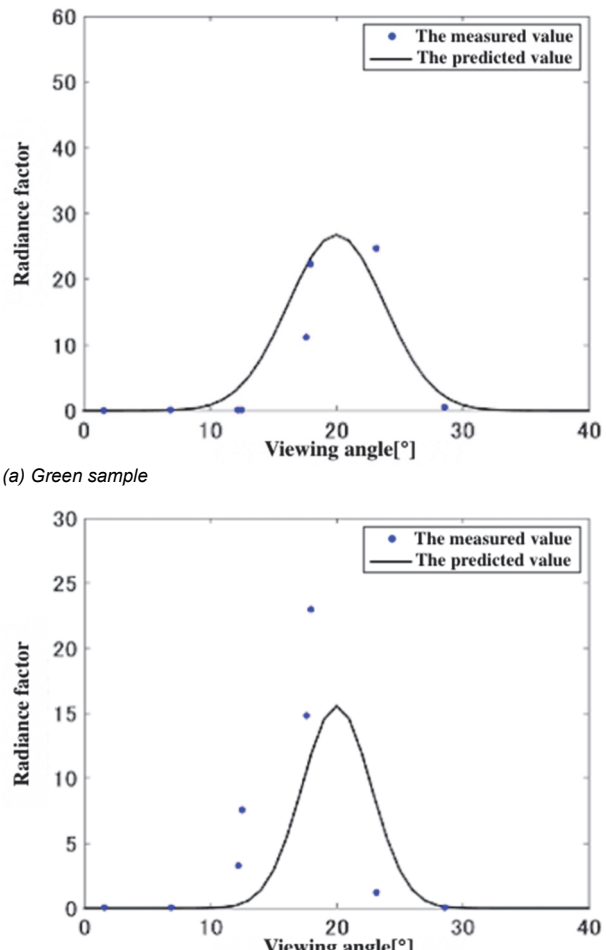


**Figure 7.** The intensity distribution of the predicted value of the model and the measured value for output angle: (a) green sample at the incident angle of  $20^\circ$  and the wavelength of 580nm, and (b) blue sample at the incident angle of  $20^\circ$  and the wavelength of 470nm

Figure 7 shows the intensity distribution of the green sample at the incident angle of  $-20^\circ$  and the wavelength of 580 nm and the intensity distribution of the blue sample at the incident angle of  $-20^\circ$  and the wavelength of 470 nm. From Fig.7, the predicted value of the model is lower than the measured value. Also, the Gaussian function theoretically shows a symmetrical distribution, but the distribution of the measured value shows a bilaterally asymmetrical distribution. From the above results, it can be considered that both the measurement accuracy is not sufficient, and the model is not appropriate. In terms of measurement accuracy, alignment of the sample, the light source, and the camera is simple so that the highest measured radiance factor may deviate from an angle of regular reflection. Therefore, in order to make the measurement more precise, it is necessary to improve the measurement accuracy by using an optical system. In terms of model, a Gaussian function with a peak near regular reflection was used, but since the sample used this time is a stainless-steel oxidation color with a sizeable specular reflection component, improvements such as using metal CG models for better approximation accuracy are needed. This time, we performed Gaussian fitting for each wavelength. However, in order to consider a reproduction model of more arbitrary structural colors, it is necessary to select a model that has arguments such as incident angle, viewing angle, wavelength, refractive index, and so on. Also, considering the relationship between a fitting accuracy and the number of measurement points, we would like to consider a simple and highly accurate measurement-model fitting.

## Reproduction of structural colors on planar surface

The structural colors were reproduced using a spectral projector [10]. Based on the measured radiance factor of the samples, we simulated and reproduced the appearance of the structural color surface under a xenon lamp, which is a base light source of the spectral projector. The reproduction for a planar surface was performed for each specific incident and viewing angles. As shown in Fig.8, it was a simple plane projection on a white plate as a screen, and a projected image is a uniform.

Figure 9 shows the reproduced spectral radiance. The incident angle in Fig.9 for green and blue samples is  $15.0^\circ$  and  $12.5^\circ$ , respectively. When reproducing structural colors of a stainless surface, there is a significant difference between radiance intensity near regular reflection and far from regular reflection. Therefore, if the scale of the light source is adjusted to the intensity of angles near regular reflection, the scale of the light source at angles far from regular reflection becomes almost zero. Thus, we reproduced viewing angles of the green sample at  $12.0^\circ$  and  $17.3^\circ$ , and those of the blue sample at  $9.1^\circ$ ,  $14.5^\circ$ , and  $19.9^\circ$ .

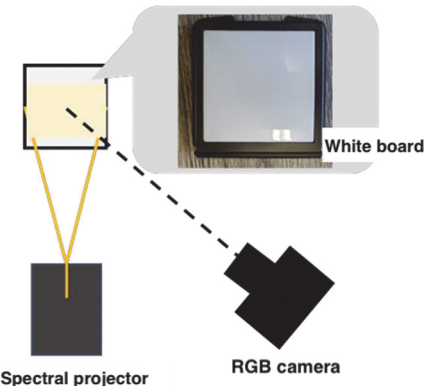


Figure 8. Reproduction environment for a planar surface

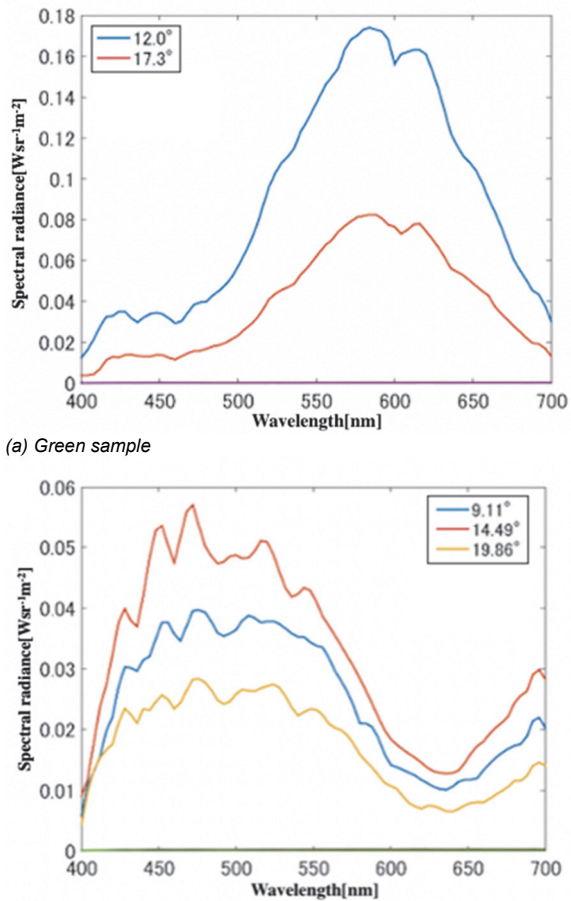


Figure 9. Reproduced spectral radiance on planar surface: (a) green sample for various viewing angles at the incident angle of  $15^\circ$ , and (b) blue sample for various viewing angles at the incident angle of  $12.5^\circ$

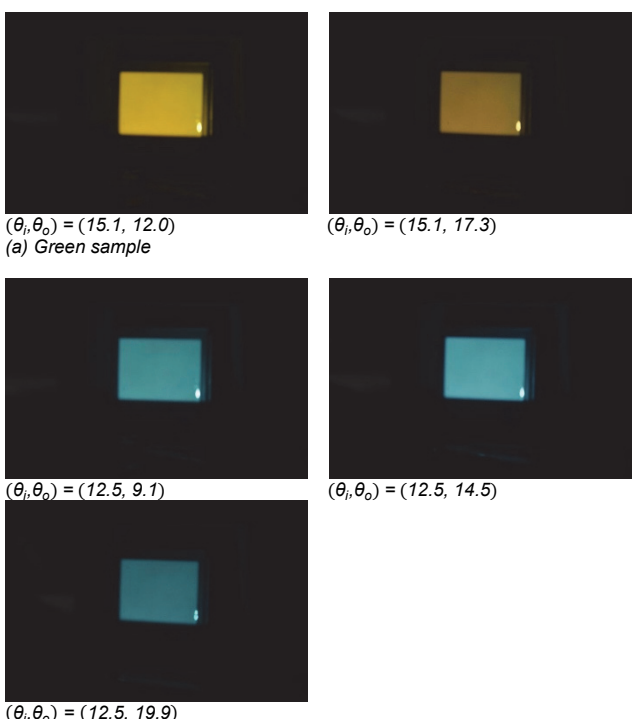


Figure 10. Result of structural color reproduction at each angle

Figure 10 shows the results of structural color reproduction for each angle. From Fig.10, different colors (brightness) can be reproduced depending on the angles. Colors close to the spectral distribution in Fig.9 can be reproduced at angles near regular reflection.

## Conclusions

In this paper, we measured a reflection characteristic of structural colors using a conventional image-based BRDF measurement method using a spectral camera. Based on the calibrated geometrical setting, we measured the angular dependence of the structural color, in which the reflectance increases as it approaches regular reflection. However, due to the angle sampling and the limitations of the shape of the measurement object, this method must be extended to measure various types of structural colors. In model fitting, the Gaussian function was fitted. However, the approximation accuracy of the measured values of angles near regular reflection was not very good due to the problems of measurement accuracy and model suitability. Also, the structural colors were reproduced for each incident angle and viewing angle. From the results, we reproduced a difference in color (brightness) depending on angles, and it can be confirmed that the color becomes brighter as it approaches regular reflection. However, structural colors are usually perceived spatially in various incident illumination directions (observation angles), so it is necessary to perform measurements with more complicated illumination conditions and observation angles.

As future work, it is necessary to select a fitting model that can approximate actual measurement data obtained by simple image-based optical characteristic measurement and improve parameter estimation accuracy. For achieving this, we would like to investigate the relationship between the accuracy of model fitting and the required optimum number of measurements and aim to reproduce angular sampling with a smaller number of measurements. Furthermore, we would like to consider a measurement method that can reproduce sample shape and optical characteristics by multiple shots and realize simple optical characteristics measurement for a structural color object of any shape. For reproduction, it is necessary to reproduce spatially different spectral distributions by more dense sampling. Therefore, we are considering reproducing in complicated irradiation direction and observation direction based on optical characteristics complemented by measurement and model fitting. Also, we would like to increase the number of structural color samples and increase measurement data of optical characteristics and variation of reproduction.

## Acknowledgments

This work was supported by JSPS KAKENHI Grant Number JP18K11347 (Grant-in-Aid for Scientific Research(C)).

## References

- [1] D.Guarnera, G.C.Guarnera, A.Ghosh, C.Denk, and M.Glencross, “BRDF Representation and Acquisition”, COMPUTER GRAPHICS forum, Vol.35, Issue.2, (2016)
- [2] W.Matusik, H.Pfister, M.Brand, and L.McMillan, “A Data-Driven Reflectance Model”, SIGGRAPH’03: ACM SIGGRAPH Papers 2003, (2003)
- [3] A.Ngan, F.Durand, and W.Matusik, “Experimental Analysis of BRDF Models”, EGSR’05: Proceedings of the Sixteenth Eurographics conference on Rendering Techniques, (2005)
- [4] Y.Kobayashi, T.Morimoto, I.Sato, Y.Mukaigawa, and K.Ikeuchi, “BRDF Estimation of Structural Color Object by Using Hyper Spectral Image”, IEEE International Conference on Computer Vision Workshops, (2013)
- [5] N.Okada, D.Zhu, D.Cai, J.B.Cole, M.Kambe, and S.Kinoshita, “Rendering Morpho butterflies based on high accuracy nano-optical simulation”, Journal of Optics, Vol.42, Issue.1, (2013).
- [6] L.Belcour and P.Barla, “A Practical Extension to Microfacet Theory for the Modeling of Varying Iridescence”, ACM Transactions on Graphics, Vol.36, No.4(65), (2017).
- [7] S.Werner, Z.Velinov, W.Jakob, and M.B.Hullin, “Scratch iridescence: Wave-optical rendering of diffractive surface structure”, ACM Transactions on Graphics, Vol.36, No.6(207), (2017)
- [8] T.Auzinger, W.Heidrich and B.Bickel, “Computational Design of Nonstructural Color for Additive Manufacturing”, ACM Transactions on Graphics, Vol.37, No.4(159), (2018)
- [9] A.Sole, I.Farup, P.Nussbaum and S.Tominaga, “Bidirectional Reflectance Measurement and Reflection Model Fitting of Complex Material Using an Image-Based Measurement Setup”, Journal of Image, Vol.4, No.11, (2018).
- [10] K.Hirai, D.Irie, T.Horiuchi, “Multi-primary Image Projector Using Programmable Spectral Light Source”, J.Soc.Inf.Display, Vol.24, Issue.3, (2016).

## Author’s Biography

Kazuki Iwata is currently a student of a bachelor’s course program in the Department of Imaging Sciences, Chiba University. His research interests are material appearance reproduction and spectral imaging technologies. Especially, he is now constructing a structural color measurement and reproduction using spectral cameras and projectors.